System Identification and Seismic Assessment Modeling Implications for Italian School Buildings

Gerard J. O'Reilly, Ph.D.[1]; Daniele Perrone, Ph.D.[2]; Matthew Fox, Ph.D.[3]; Ricardo Monteiro, Ph.D.[4]; Andre Filiatrault, Ph.D., M.ASCE[5]; Igor Lanese, Ph.D.[6]; and Alberto Pavese, Ph.D.[7]

Abstract: Extensive damage to school buildings has been observed during past earthquakes in Italy, with the 2002 Molise earthquake resulting in the complete collapse of a school building, leading to numerous casualties. In this paper, data provided by instruments installed in a number of school buildings throughout Italy from both ambient vibration and triggered dynamic vibration following the 2016 Central Italy earthquake are compared with predictions of numerical models. This comparison of predicted and measured structural response characteristics is investigated to provide practicing engineers with further insight into and validation of the accuracy of typical modeling techniques compared with instrumented responses of numerous different building typologies subjected to different dynamic excitations. Initial comparisons demonstrate reasonable agreement between the numerically predicted modes of vibration and natural frequencies from ambient vibration measurements, with further numerical parametric studies exhibiting improved matching. Additional comparative analyses are considered to discuss the potential impacts on the seismic assessment of existing structures within a performance-based seismic assessment framework. **DOI: 10.1061/(ASCE)CF.1943-5509.0001237.**

Author keywords: Seismic assessment; Instrumentation; Modeling; School buildings.

Introduction

The collapse of the Iovene primary school in San Giuliano during the Molise 2002 earthquake, which killed 27 students and their teacher, highlighted the seismic vulnerability of the existing Italian school building stock. With this in mind, the European Centre for Training and Research in Earthquake Engineering (EUCENTRE) initiated a research project entitled Progetto Scuole in 2015, with the main objective of seismically assessing a number of school buildings throughout Italy that were considered to be representative of the overall stock. Considering past studies of seismic assessment and risk mitigation, such as the Seismic Project Identification Report (SPIR) Guidelines in British Columbia, Canada (SPIR 2014), this project aimed to apply some of the more recent advancements in performance-based seismic assessment through the application of guidelines, such as FEMA P58 (FEMA 2012), to existing Italian school buildings. Extensive analyses were conducted to aid more-informed decisions regarding both structural retrofitting to prevent collapse and ways to mitigate the extensive monetary losses due to the cost of repairing structural and nonstructural elements (O'Reilly et al. 2018). Furthermore, numerous accelerometers were installed at each school location to characterize the ambient response and compare it with the predictions of the numerical models developed, in addition to capturing any triggered seismic response in the event of a nearby earthquake. This paper also outlines this latter aspect, whereby the modal response measured during ambient vibrations is compared with that identified from numerical models developed following in situ surveying for seismic loss estimation studies. This is performed for various building construction typologies typically found throughout Italy, such as RC frames with masonry infill, unreinforced masonry (URM), and precast (PC) RC frames. A parametric study is conducted to compared numerically some of the key factors in predicted dynamic characteristics with those identified from the ambient vibration recordings. Furthermore, recordings from three triggered vibrations at one of the school buildings during the 2016 Central Italy earthquake are also evaluated to provide further insight into the comparisons between in situ instrumentation and numerical modeling. The observations from both the ambient and triggered vibrations are then discussed further with additional numerical analysis that highlights some of the potential implications of the different numerical modeling decisions for assessment within a performance-based earthquake engineering framework.

[1]Postdoctoral Researcher, Centre for Understanding and Managing Extremes, Scuola Universitaria Superiore IUSS Pavia, Palazzo del Broletto, Piazza della Vittoria 15, Pavia 27100, Italy (corresponding author). ORCID: https://orcid.org/0000-0001-5497-030X. Email: gerard.oreilly@iusspavia.it

[2]Postdoctoral Researcher, Centre for Understanding and Managing Extremes, Scuola Universitaria Superiore IUSS Pavia, Palazzo del Broletto, Piazza della Vittoria 15, Pavia 27100, Italy.

[3]Senior Engineer, Beca Limited, 267 High St., Christchurch 8011, New Zealand.

[4]Assistant Professor, Centre for Understanding and Managing Extremes, Scuola Universitaria Superiore IUSS Pavia, Palazzo del Broletto, Piazza della Vittoria 15, Pavia 27100, Italy.

[5]Professor, Centre for Understanding and Managing Extremes, Scuola Universitaria Superiore IUSS Pavia, Palazzo del Broletto, Piazza della Vittoria 15, Pavia 27100, Italy; Professor, Dept. of Civil, Structural, and Environmental Engineering, State Univ. of New York, Buffalo, NY 14260.

[6]Research Collaborator, European Centre for Training and Research in Earthquake Engineering, via Adolfo Ferrata 1, Pavia 27100, Italy.

[7]Professor, Dept. of Civil Engineering and Architecture, Univ. of Pavia, Pavia 27100, Italy; Research Collaborator, European Centre for Training and Research in Earthquake Engineering, via Adolfo Ferrata 1, Pavia 27100, Italy.

Note. This manuscript was submitted on January 23, 2018; approved on July 13, 2018; published online on November 8, 2018. Discussion period open until April 8, 2019; separate discussions must be submitted for individual papers. This paper is part of the ***Journal of Performance of Constructed Facilities***, © ASCE, ISSN 0887-3828.

Table 1. General information for selected case study school buildings

School	Region	Typology	No. of stories	Construction period
Ancona	Marche	RC	3	1960s
Avola	Sicilia	URM	2	1900s
Carrara	Toscana	RC	2	1960s
Cassino	Lazio	PC	2	1980s

Survey of School Buildings

As part of Progetto Scuole, a total of six school buildings with different structural typologies were selected for detailed evaluation and analysis. Available information from over 49,000 Italian school buildings (Borzi et al. 2011) was collected and used to determine the predominant characteristics of the existing scholastic building stock (e.g., number of stories, construction typology, age, and so on). Using this information, a sample of buildings representative of the entire stock could be established and examined in more detail while also remaining feasible from a practical and economic point of view. This information showed that (1) the majority of scholastic structures consist of three or fewer stories, (2) are usually constructed of RC frames with unreinforced masonry infills, and (3) the older the structure is, the more likely it is to be constructed with URM. Furthermore, around 67% of existing school buildings in Italy were constructed before 1975, which corresponds to the introduction of modern seismic design provisions in Italy. With these considerations, Table 1 lists four of the final six school buildings chosen at various locations throughout Italy for this study to be representative of the typical school building characteristics (Borzi et al. 2011). O'Reilly et al. (2017) provided information on all six buildings; only four are discussed here due to space limitations. Their locations are illustrated in Fig. 1 alongside the most recent hazard map of Italy (Montaldo and Meletti 2007).

In situ surveys were conducted to characterize the structural configurations in addition to the nonstructural elements so that detailed numerical models could be developed and loss estimation studies carried out. Fig. 2 illustrates the main information related to the structural configurations of the four case study buildings. The URM school building in Avola is characterized by two floors, with interstory heights of 3.95 and 4.35 m for the first (ground) and second floors, respectively, and a plan dimension of 47×12 m. The masonry walls are made of limestone with thickness varying between 0.85 and 0.40 m [Fig. 2(b)].

The RC schools located in Ancona and Carrara are illustrated in Figs. 2(a and c), respectively. RC frame members typically

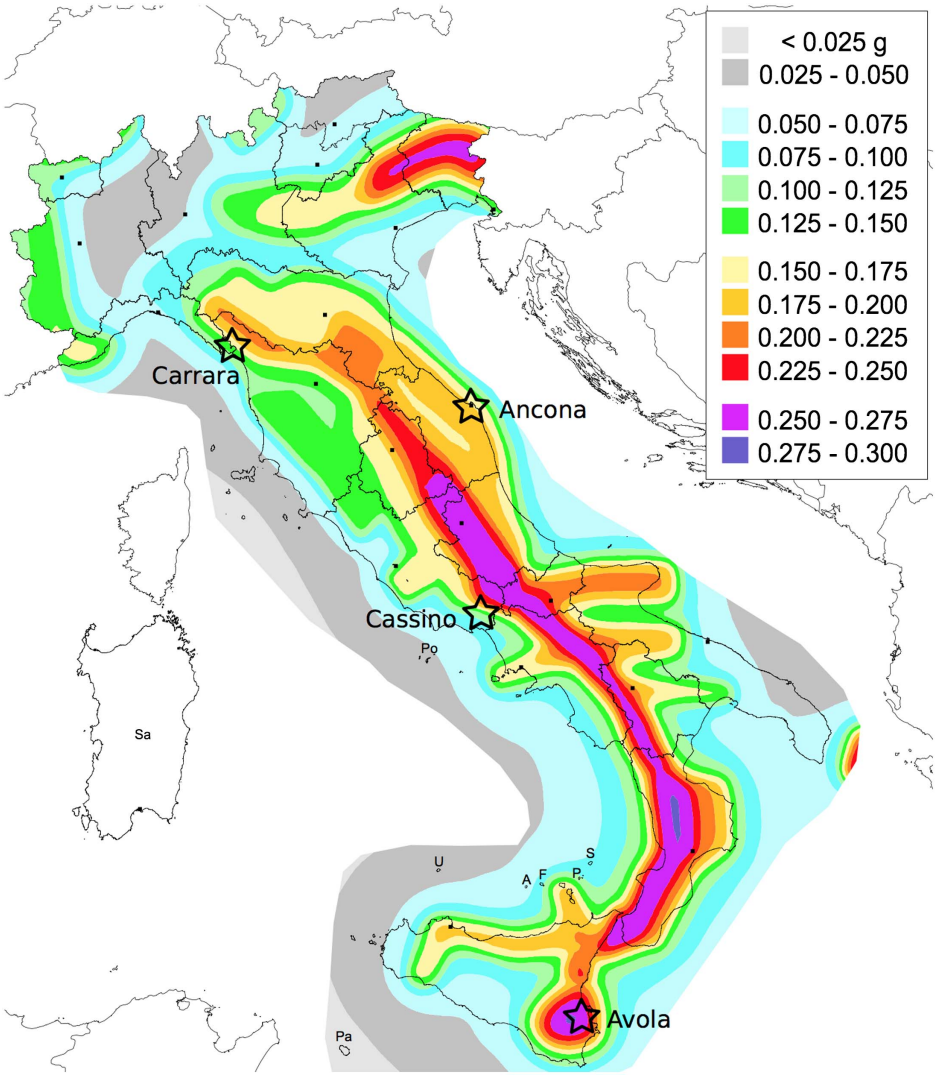

Fig. 1. Location of each school building with respect to Istituto Nazionale di Geofisica e Vulcanologia (INGV) 475-year return period hazard map for peak ground acceleration. (Data from INGV 2017.)

J. Perform. Constr. Facil., 2019, 33(1): 04018089

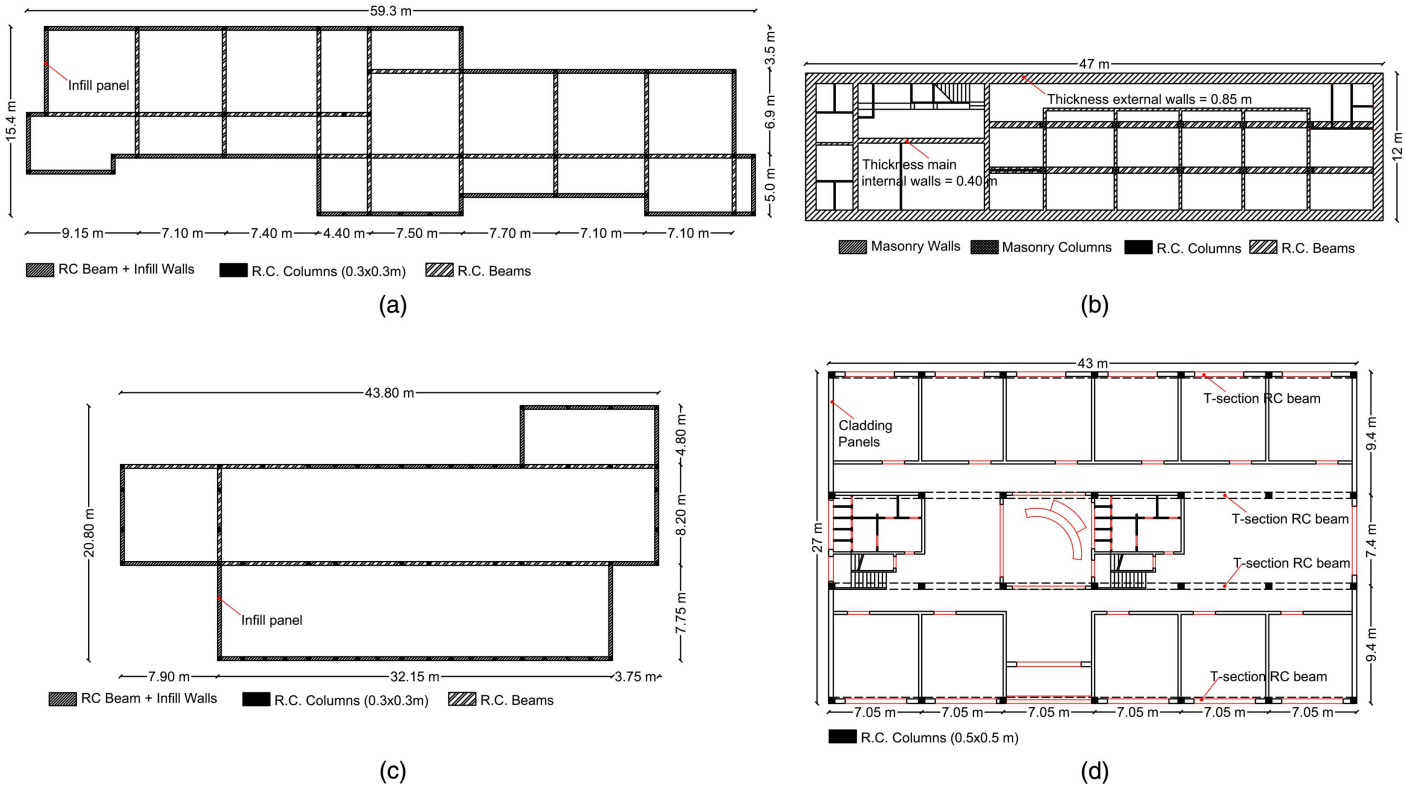

Fig. 2. Main geometrical and structural properties of case study buildings: (a) Ancona; (b) Avola; (c) Carrara; and (d) Cassino.

consist of 30-cm-square columns and 30×50-cm beams that were designed for gravity loads only. Infills were identified as double-leaf 12-cm hollow clay brick with a 5-cm-wide internal cavity. The floor systems were identified as laterizio floor systems (Bacco 2009) that were quite common in Italy at the time. In the case of the PC school building illustrated in Fig. 2(d), the structural system comprises precast columns supporting precast beams in the longitudinal direction only. The beam members support a precast hollow-core floor system with a thin in situ topping spanning the transverse direction.

Instrumentation and Data Acquisition and Processing

The reliable numerical modeling of an existing building can be generally enhanced through the tuning of some parameters based on experimental and in situ measurements. Typically, uncertainties associated with material properties, reinforcing bar locations, and concrete properties can be reduced through experimental investigation, whereas the impacts of modeling uncertainty on the response assessment can be incorporated using the results of studies such as O'Reilly and Sullivan (2017b, 2018b), among others. To this extent, each selected school building was equipped with an advanced structural monitoring system aimed at continuous dynamic system identification through ambient vibration acquisitions. These instruments were scheduled to record 1-min snapshots of the ambient vibration daily, with which to identify the modal properties. In addition, the monitoring system was designed to record possible seismic events when a predetermined acceleration threshold of $0.015g$ was exceeded at the base of the building. In the event of triggered recording, a predefined routine ensured the acquisition of the whole seismic event, including 30 s of preceding data included in a temporary buffer.

Each school building was instrumented with state-of-the-art high-quality SARA (Perugia, Italy) sensors. The SARA SA10 (SARA Electronic Instruments 2018) are force-balance $1g$ biaxial accelerometers, using a 12V DC power supply, with $10\text{V}/g$ sensitivity with differential output, nonlinearity <0.1%, and hysteresis <0.001% over the full range, with measurable frequency up to 200 Hz. These instruments are suitable for recording both ground motions and ambient vibrations. One reference accelerometer was installed at the lowest floor slab of each school building [e.g., Fig. 3(a) for the Ancona school building], whereas two accelerometers were installed at the highest floor level accessible, e.g., the RC slab at the roof level for the Ancona school building [Fig. 3(b)]. Each sensor was fastened to the structure with a posttensioned steel bolt [Fig. 3(a)] and its orientation aligned with the principal orthogonal directions of each building. This sensor configuration is generally sufficient to measure the first few vibration modes of most typical buildings. Higher modes, particularly in low-rise buildings, are generally very difficult to recognize experimentally and do not provide as much useful information compared with the first few modes of vibration.

The data acquired from both ambient and triggered vibrations was transmitted in real-time to the EUCENTRE cloud server through a Universal Mobile Telecommunications System modem, and automatic postprocessing software was implemented. The procedure for the frequencies and mode shapes identification was as follows: for each scheduled acquisition, with a default sampling rate of 128 Hz and duration of 60 s, the discrete Fourier transform (DFT) (Bonetto 2013) between the channels of the two accelerometers located on the top of the structure was computed. Once the DFT was obtained, the enhanced frequency domain decomposition (EFDD) method was applied (Vincenzi 2007; Islami 2013). In this process, the singular value decomposition (SVD) was used to separate the contribution of each vibration mode, switching from an n-degrees-of-freedom (DOF) system to n single-DOF

(a) (b)

Fig. 3. Accelerometer installation for Ancona school building: (a) reference accelerometer at slab on grade; and (b) top floor slab location of accelerometers for dynamic identification.

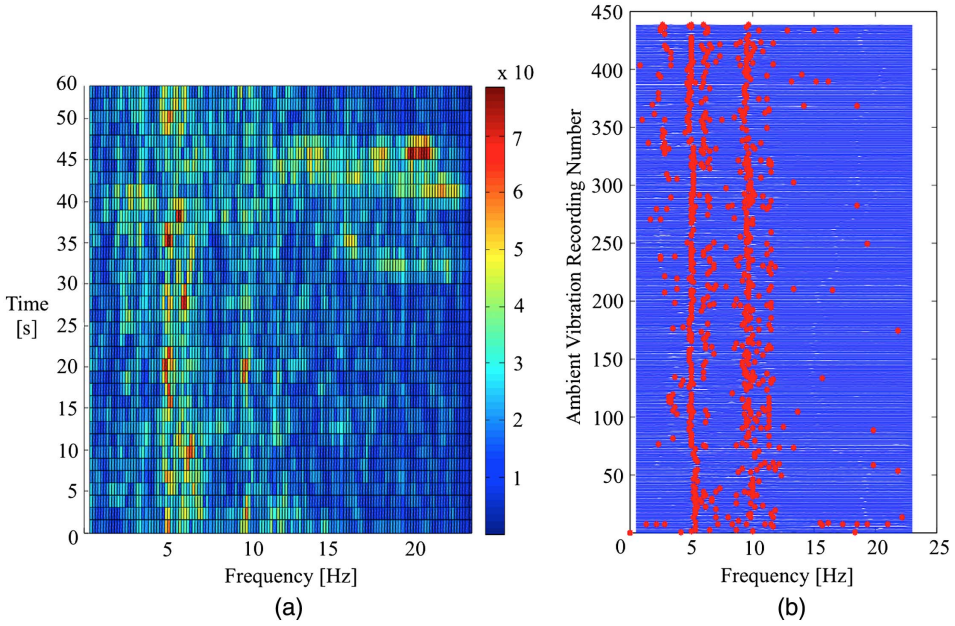

(a) (b)

Fig. 4. Output of processed continuous dynamic identification with (a) identification of frequencies for a single measurement by analyzing amplitude of different frequencies over duration of ambient vibration recording; and (b) numerous measurements with identified frequencies stacked together to identify the overall trend of different ambient vibration measurements.

systems. On the SVD curve, the peak picking (PP) method (Rainieri et al. 2009a, b; Piovesan 2013) was applied to identify the modal frequencies for each acquisition. Further checks were then also applied to remove spurious peaks from the real identified modal frequencies (Magalhães et al. 2012). Fig. 4(a) shows an example of the identification of the natural frequencies for a single 60-s-interval ambient measurement. The data indicated a high amplitude around 5 Hz. Using the information from many of these 60-s windows for frequency identification, a more general plot to illustrate the overall trend in frequencies using the results of numerous ambient vibrations is shown in Fig. 4(b).

The output of the implemented automatic data-processing procedure still showed some data scatter, although a trend of certain recurring frequencies was certainly observed. For example, Fig. 4(b) shows a repeated identification of two potential mode shapes at around 5 and 10 Hz. Such information, integrated with the phase analysis of the signals and combined with the results of the numerical model, often leads to the proper experimental identification of natural frequencies and associated modes of vibrations that could then form the basis for numerical modeling evaluation and calibration.

Numerical Modeling

For each of the case study school buildings, a detailed numerical model was developed. These numerical models incorporated both effects of nonlinear material behavior and second-order geometry effects, commonly referred to as P-delta effects, to permit extensive nonlinear response-history analysis (NRHA) of each school building.

In the case of the RC frame structures with masonry infills in Ancona and Carrara (Table 1), the numerical model was developed

using the OpenSees framework (McKenna et al. 2010) based on the modeling recommendations of O'Reilly and Sullivan (2015, 2017a). This takes into account the various aspects of RC frames with masonry infill behavior constructed in Italy prior to the introduction of seismic design provisions in the 1970s, when structures were typically designed for gravity loads only using the available design (Vona and Masi 2004). Aspects such as the modified ductility of plastic hinges in frame members (e.g., Melo et al. 2012) due to the presence of smooth reinforcing bars and low levels of transverse shear reinforcement are accounted for, in addition to the vulnerability of beam-column joints due to a lack of transverse shear reinforcement that was experimentally shown by Pampanin et al. (2002), for example, to result in brittle shear failure modes through the build-up of excessive diagonal principal tensile stresses in the beam-column joint. These modeling aspects were developed based on past observations of damage in Italy (O'Reilly and Sullivan 2017a) and were incorporated directly into the modeling procedure adopted here. In situ test reports made available during the survey of the Ancona building showed the mean compressive strength of the concrete to be 14.4, 10.8, and 8.7 MPa at the first (ground), second, and third stories, respectively. Furthermore, the yield strength of the reinforcement bars was reported to be equal to 381 MPa. In the case of the school building in Carrara, no in situ test data were available, and hence reasonable values were assumed based on those observed in the school in Ancona. Hence, a value of 14 MPa was assumed for the mean compressive strength of the concrete and a value of 380 MPa was assumed as the yield rebar strength. The Young's modulus of the concrete was evaluated based on the formulation provided by Collins and Mitchell (1991) to give values of 19,500, 17,800, and 16,700 MPa for the respective strengths listed previously for Ancona, whereas a fixed value of 19,300 MPa was used for Carrara.

Furthermore, the effect of masonry infills on the overall response of the structures was incorporated using an equivalent diagonal strut modeling approach (Crisafulli et al. 2000). For both RC buildings, hollow clay bricks were adopted for the masonry infills. Unfortunately, in situ tests to assess the mechanical properties of the masonry infills were not available. For this reason, the mean properties available in the literature for double-leaf hollow clay masonry infills by Hak et al. (2012) in addition to the recommendations of Sassun et al. (2015) regarding limit-state drift limit definitions were used for both case study buildings.

The hysteretic behavior of these struts was computed using the recommendations of Sassun et al. (2015), which were based on the aggregated results of numerous different test data on the capacity of masonry infills. Lastly, staircase modeling was taken into account through equivalent elastic strut elements to account for the additional stiffness offered by these elements (Fig. 5). Shear failure of column members due to interaction with masonry infill and staircase elements has been observed during past seismic events in Italy (O'Reilly and Sullivan 2017a). To account for this, an uncoupled zero-length element was introduced at the column ends to model their limited shear capacity in addition to adopting a double equivalent masonry infill strut layout (Crisafulli et al. 2000) to model the forces transferred to the columns to account for this potential mechanism, as illustrated in Fig. 5 and discussed in further detail by O'Reilly (2016). These uncoupled zero-length elements were modeled using the shear strength model proposed by Zimos et al. (2015) to account for the potential shear failure as a result of excessive shear force transfer from the masonry infills or staircases. The floor slab system was modeled as a rigid diaphragm. Fig. 5 illustrates the main modeling aspects for the school building in Ancona, in which the various aspects discussed previously are highlighted.

The URM school building in Avola (Table 1) was modeled using TreMuri (Lagomarsino et al. 2013), which allows for the evaluation of masonry buildings. The survey allowed the main structural details required to model and analyze the building to be identified. Based on its characteristics, the concrete slabs were assumed to be rigid. Good wall-to-diaphragm connections were observed and a proper connection between the perpendicular walls was verified. With these assumptions, and also considering the in-plan and elevation regularity of the building, it is reasonable to neglect the local flexural behavior of the floors and the local wall out-of-plane response with respect to the global building response, which is governed by the in-plane behavior (Lagomarsino et al. 2013). During the in situ survey, it was not possible to perform destructive in situ measurements; hence the mean value of the mechanical properties proposed by the Italian National Code (NTC 2008)

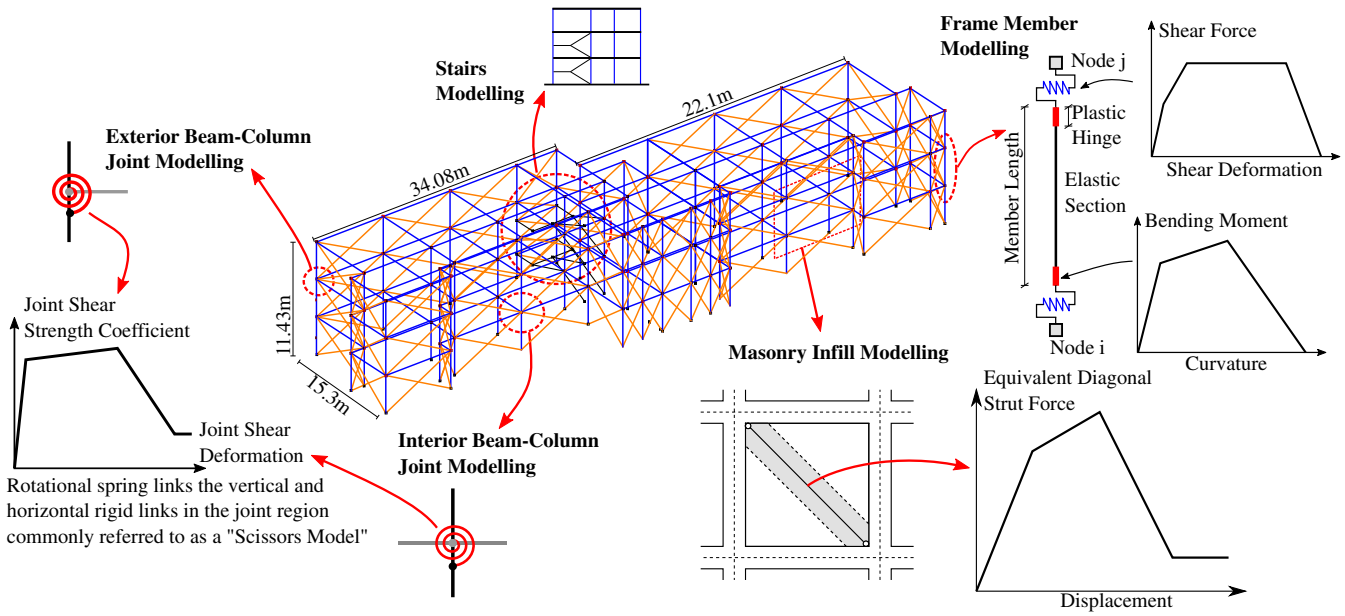

Fig. 5. Numerical model of school building in Ancona, highlighting main modeling aspects.

J. Perform. Constr. Facil., 2019, 33(1): 04018089

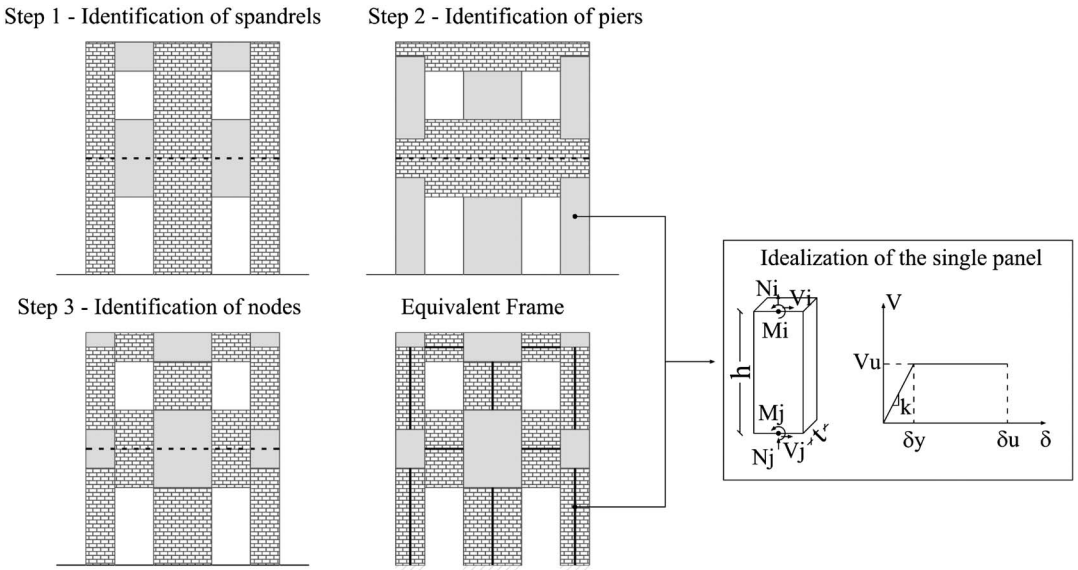

Fig. 6. Equivalent in-plane frame idealization of URM walls using TreMuri for masonry structures. (Adapted from Lagomarsino et al. 2013.)

and Eurocode 8 (CEN 2004, 2005) for limestone masonry were adopted in this study. In particular, the compressive and shear strengths and Young's modulus of the masonry were assumed to be 1.9, 0.035, and 1,080, respectively. An equivalent frame modeling approach was developed in TreMuri. Fig. 6 summarizes the steps required to define the idealized equivalent frame model consisting of spandrels, piers, and rigid nodes. The capacity of the structure is mainly related to the vertical and lateral capacity of the piers. The spandrels couple the response of adjacent piers in the case of lateral loads, and their geometry is defined based on the vertical alignment and overlap of the openings.

The behavior of the masonry panels was simulated by means of a bilinear relationship with a capping strength and a postcapping stiffness decay (for nonmonotonic action). The initial elastic stiffness is directly defined by the shear and flexural stiffness using the geometric and mechanical properties of the masonry walls. A stiffness reduction factor to account for the cracked conditions of the panels was introduced in the element stiffness matrix. This reduction factor, described in further detail by Lagomarsino et al. (2013), defined as a function of the compressive stress state of the masonry panels, was calibrated through parametric nonlinear finite-element method (FEM) analyses (Lagomarsino et al. 2013). The ultimate shear and bending strength were computed from simplified criteria that considered two different possible failure modes Lagomarsino et al. (2013): (1) flexural failure associated with the rocking and crushing of walls, and (2) shear failure related to shear sliding or diagonal cracking. For dynamic analysis, the failure of the panel was defined in terms of maximum drift limits. The drift limits were defined according to Eurocode 8 and were based on the prevailing failure mechanism occurring in the panel: 0.4% and 0.8%, respectively, for the shear failure and flexure failure. When a panel exceeded the limit and was deemed to have failed, the element became a strut with no residual shear and/or bending capacity, whereas the axial load was maintained.

Lastly, in the case of the precast school building in Cassino (Table 1), the numerical model was developed in Ruaumoko 3D (Carr 2007). Beam-column joints represented the most complex aspect of the model. To capture this, each joint was modeled using gap and friction elements (Fig. 7). The gap elements reflected the gaps between the beams and columns observed during in situ surveys of the school. The friction elements allowed for sliding of the beams seated on the column corbels. The corresponding moment capacity was computed as the frictional resistance of the beam seated on the column corbel multiplied by the lever arm, which was taken as the beam depth (Fig. 7). A lumped plasticity modeling approach was adopted for the precast RC columns. Plastic hinges were permitted to form at the top and bottom of the columns in both stories should sufficient bending moment be generated; the plastic hinge length was calculated in accordance with Paulay and Priestley (1992). Available information following the building survey was used to identify the mean compressive strength of the concrete as 25 MPa and the Young's modulus as 23,500 MPa. The gap elements at the beam-column connection were set with a 20-mm initial gap based on in situ measurements, and a friction coefficient of 0.40 was assumed. Considering the limited strength of the beam-column joints, because they consist of a seated connection, it was deemed unlikely that plastic hinges would form in the beams and

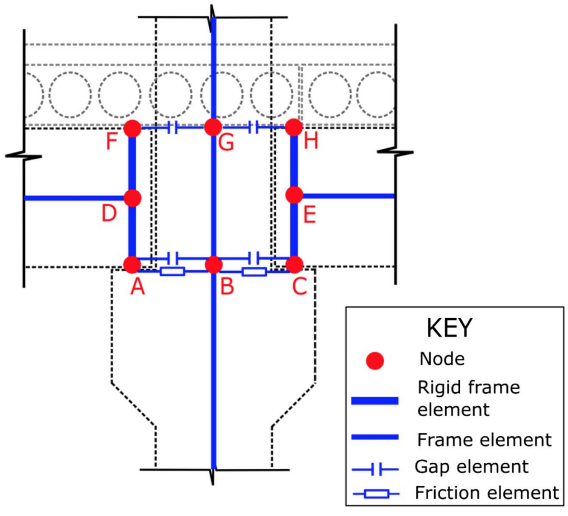

Fig. 7. Numerical modeling of PC building beam-column joint connection which consisted of beam members seated on column corbels using gap and friction elements.

they were therefore modeled as linear elastic frame elements. The shear behavior of all members was modeled as linear elastic. A significant reduction in shear stiffness would be expected as a RC section begins to crack and yield, but this reduction was not accounted for because preliminary studies determined that the total shear deformations were negligible relative to flexural deformations. The precast floor topping is relatively thin, and it was therefore decided to explicitly model the flexibility of the diaphragms rather than assume a rigid diaphragm. Precast floor units were modeled individually; however, sensitivity analyses found that in reality this had little impact on the response compared with the assumption of a rigid diaphragm. Finally, the columns were assumed to be fixed at the base of the building.

Comparison of Measured Modal Properties with Numerical Model Predictions

Initial Comparison with Ambient Vibration Measurements

Using the modal properties of both the numerical models and the instrumentation described in previous sections, the two sets of results were compared to gauge how well the models represented the modal properties of the school buildings. These were compared in terms of the overall mode shape and natural frequency of the first few modes of vibration. At this stage, the numerical models provided blind predictions of the dynamic characteristics of the buildings, with no calibration based on experimental data.

Fig. 8(b) illustrates the data obtained from a single ambient vibration recording for the Ancona school building, in which the transfer function was produced and the modes of vibration identified through the dots plotted at the function's local frequency peaks. Fig. 8(a) shows a number of these transfer functions and their associated modal peaks condensed onto a single plot. A clear trend in the modal properties between different ambient vibration recordings can be identified, as previously noted for Fig. 4.

To better illustrate this, the natural frequencies identified for each ambient vibration recording (the dots) were compiled and plotted in histogram format (Fig. 9) for the case of the school in Ancona. This process clearly illustrates the frequency range in which the identified frequencies tended to fall. In addition, the natural frequencies for each mode identified by the acquisition system are also illustrated by the vertical dashed line. The single set of values identified by the data acquisition system was determined by considering the peaks identified from different transfer functions, as outlined in Fig. 8(b), and by taking the geometric mean of the first four modes identified. The geometric mean was used to avoid adverse influence by instances of spurious mode identification, which can be observed in some cases in Fig. 8(a), and to be representative of the overall trend in the data.

Using each of the identified natural frequencies from the data acquisition system at each school, Table 2 compares the predictions of the numerical models for each school building. As is

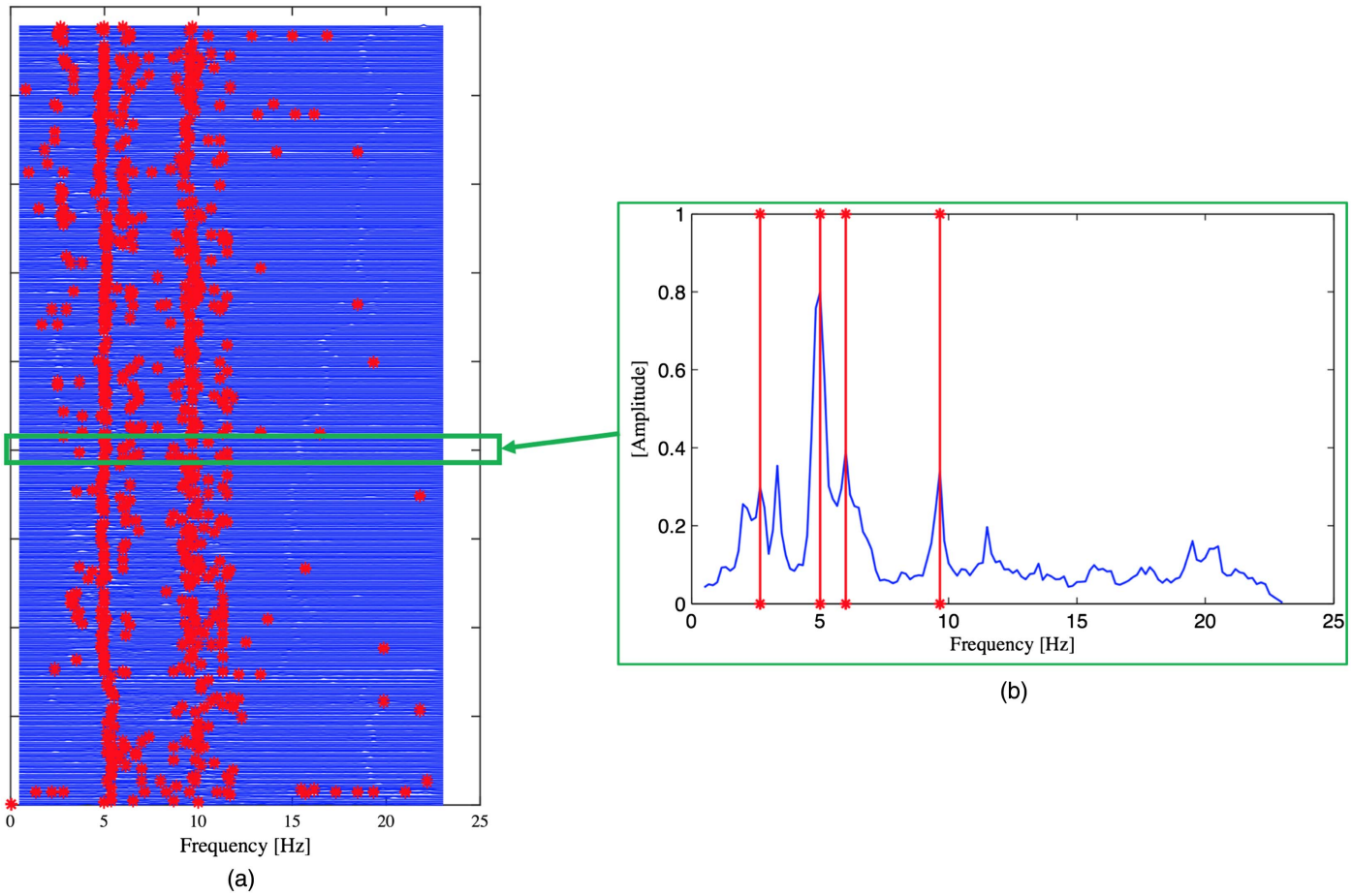

Fig. 8. Single transfer function from ambient vibrations recorded at school building in Ancona: (a) stacked plot of transfer functions from all ambient vibration measurements (dots = identified peaks); and (b) modes of vibration identified by data monitoring system.

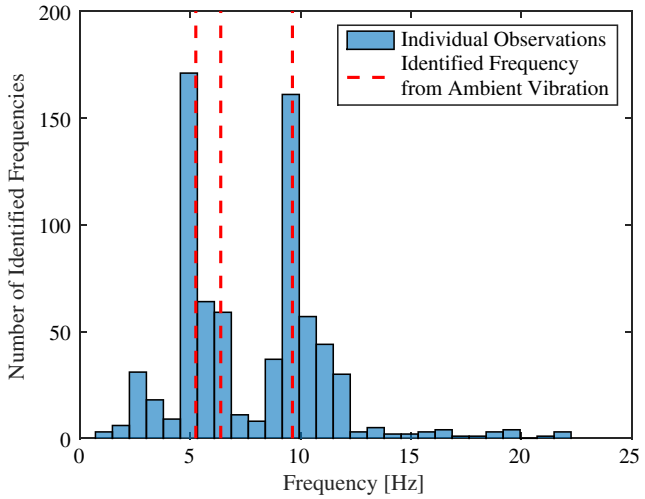

Fig. 9. Natural frequencies identified from ambient vibration recordings.

immediately obvious, the numerical model predictions and the identified modal properties from ambient vibration differed substantially. The natural frequencies reported from the ambient vibration tended to be higher. However, the modes of vibration corresponded well with those reported by the instrumentation (see Fig. 10 for the Ancona school building), indicating that the relative distribution of mass and stiffness in the numerical models is representative, but the actual values led to a discrepancy in the natural frequencies. Because the natural frequencies are related to both the seismic weight and stiffness of the structure, these were investigated further. However, because the seismic weight of the buildings can be reasonably well computed from the floor loading and self-weight of the building, the preceding discrepancy indicates that the initial stiffness values were too low in the models. This was furthered by the fact that initial parametric studies in which the floor gravity loading was both increased and reduced had negligible effects on the predicted natural frequencies compared with the variations in element stiffness. As such, only a variation in initial stiffness of the structural models was explored further.

In the case of the Cassino school building, a significant discrepancy between the predicted and measured frequencies was observed compared with the other school buildings. Further examination of the data obtained from the instruments did not show a clear trend as in the case of the Ancona buildings in Fig. 8. It was deemed that this lack of quality information arose due to the positioning of the instruments. Because of lack of access to the roof level, the two instruments were placed at the highest point of two columns at different ends of the top floor level. This was also done in other schools where access to the roof level was not possible. However, in the case of the PC Cassino school building, a rigid diaphragm was not present. It was suspected that the combination of the connection of the beams seated on the column corbels and the lack of rigid diaphragm action to force the different structural elements to move in unity resulted in some relative movement, and, as a result, a poor trend in the ambient vibration recordings to identify the modal properties relative to the other school buildings.

Parametric Study

From the initial comparison of the measured and predicted natural frequencies of the buildings listed in Table 2, the numerical models predicted lower natural frequencies than the ambient vibration measurements. To investigate further, a parametric study was conducted to examine some of the numerical parameters that may have caused such differences. This was conducted for each of the building typologies, for which the different modeling decisions likely to influence the modal properties were identified and justification for their variations provided.

In the RC frame school buildings, two sources of stiffness that were examined in detail were the RC frame elements (i.e., beams and columns) and the masonry infills. As outlined previously, one of the assumptions regarding the initial stiffness of the frame elements was that a cracked section stiffness was adopted in the flexural behavior model (O'Reilly and Sullivan 2017a). This approach is widely adopted in design and assessment, with Eurocode 8 (CEN 2004, 2005) recommending a cracked section stiffness ratio of 50% be adopted in the absence of more-detailed information. However, in the critical review by Priestley (1993, 2003), the recommendation for the cracked section stiffness ratio was shown to be much less than 50% in cases of relatively low levels of longitudinal reinforcement and axial load, aspects that are quite prevalent in RC frames designed before the 1970s in Italy. Priestley highlighted how errors in initial stiffness of the frame members such as beams and columns undoubtedly result in erroneous modal analysis, and recommended that a more representative value of the cracked section stiffness be determined from moment-curvature analysis. The following must then be determined: (1) the extent of cracking in the frame members in each of the school buildings, and (2) how much of an impact the differences in fully cracked section stiffness and gross section stiffness actually have on the modal analysis results.

Table 2. Natural frequencies reported from ambient vibration measurements and predicted using numerical modeling

School	Typology	Mode	Mode shape	Effective modal mass (%)	Natural frequency (Hz)		Measured/predicted
					Predicted	Measured	
Ancona	RC	1	Translational	41.2	1.61	5.25	3.3
		2	Lateral-torsional	0.30	2.24	6.38	2.8
		3	Translational	42.6	2.74	9.63	3.5
Carrara	RC	1	Translational	39.4	1.45	4.50	3.1
		2	Lateral-torsional	39.0	2.34	5.13	2.2
		3	Lateral-torsional	9.00	2.47	6.38	2.6
Avola	URM	1	Lateral-torsional	87.2	2.31	5.21	2.3
		2	Lateral-torsional	12.7	4.35	17.5	4.0
Cassino	PC	1	Lateral-torsional	35.0	0.84	7.5	8.9
		2	Lateral-torsional	32.5	0.86	17.8	20.7

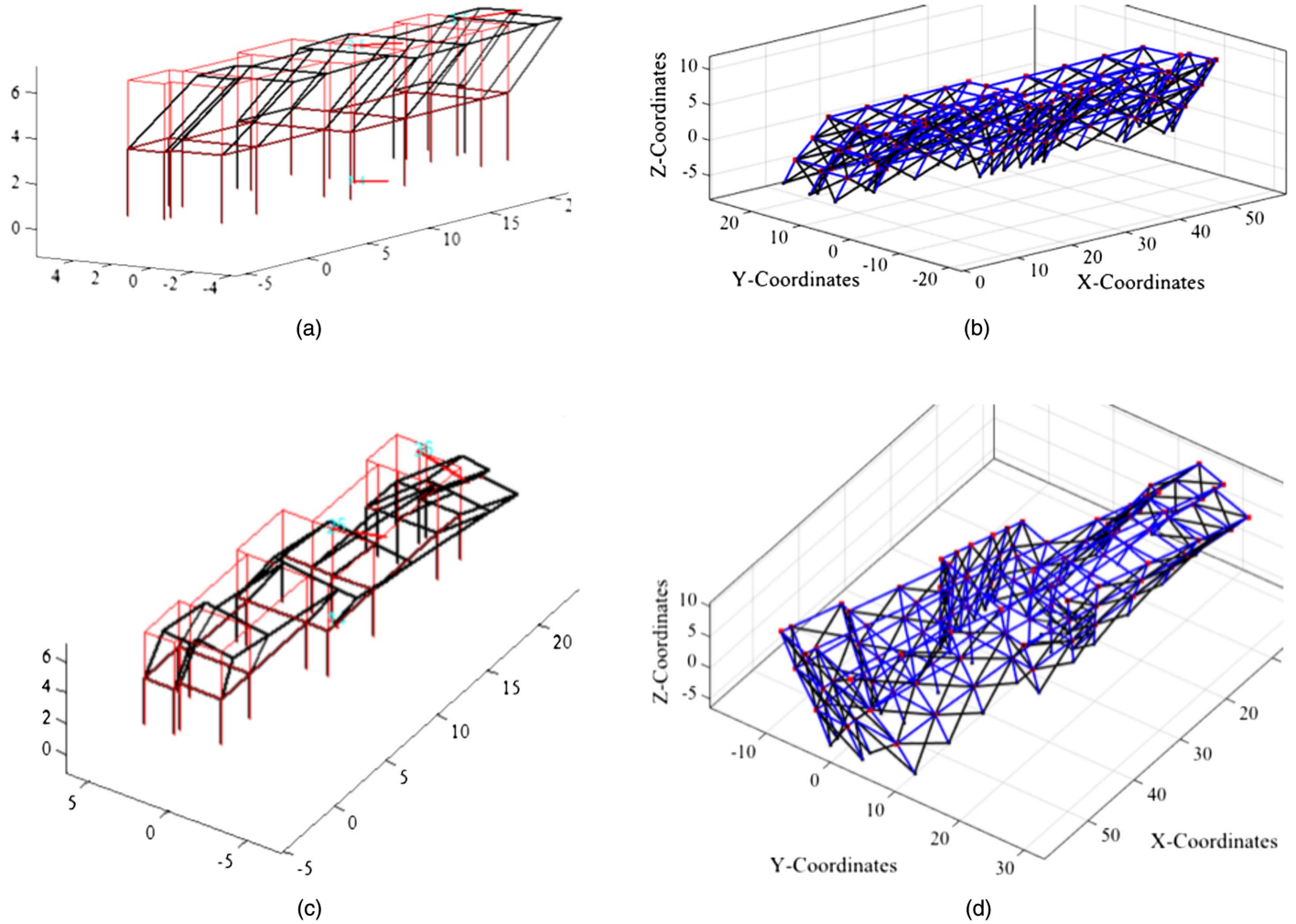

Fig. 10. Example of agreement between first two mode shapes of school building in Ancona, in which lateral-torsional coupled mode shapes are evident in both cases: (a) ambient vibration first-mode shape identified by data acquisition system; (b) first-mode shape predicted from eigenvalue analysis by numerical model; (c) ambient vibration second-mode shape identified by data acquisition system; and (d) second-mode shape predicted from eigenvalue analysis by numerical model. Lack of modal displacements at intermediate floors for modes identified by data acquisition system are due to instruments being placed at roof level only.

To illustrate the progression between cracked and uncracked RC section properties, the evolution of the natural frequencies of vibration over time during the experimental testing of a three-story RC frame test specimen (Negro 2005) is illustrated in Fig. 11. This test specimen is referred to as the seismic performance assessment and rehabilitation of existing buildings (SPEAR) building and consisted of a three-story RC frame designed to resist vertical gravity load only and without capacity design principles that form the basis of modern seismic design codes. Negro (2005) described the full-scale specimen without masonry infills tested using pseudodynamic testing at the European Laboratory for Structural Assessment (ELSA) in Ispra, Italy in 2004. The structure was doubly asymmetric, meaning that torsional response was expected to be significant. The test specimen was bidirectionally excited with four actuators; further details of the test setup were provided by Molina et al. (1999).

During the testing reported by Negro et al. (2004), the natural frequencies of the first three modes of vibration were monitored in order to examine the influence of the damage on the modal properties. Comparing the natural frequencies showed that at the beginning of the test, the cracked section stiffness model built using the same modeling techniques adopted here tended to underestimate the natural frequency, whereas the elastic model tended to overestimate. In fact, while transporting the specimen into position to be tested from outside the laboratory where it was built, some minor cracking of the elements was noted. This slight initial cracking of the test specimen further explains the slight overestimation of the natural frequencies when using an elastic section stiffness model. However, as the test progressed and the sections began to crack, the modal properties gradually moved toward the cracked model's frequency before decreasing even further as the structure entered the nonlinear range of response. This is clear in Fig. 11 for the modal properties recorded in the interval between 5 and 10 s of the test, when the natural frequencies predicted by the cracked section stiffness model corresponded very well with the observed values. Comparing these natural frequencies, an interesting observation can be made. At the beginning of the test, when the test specimen was deemed to be relatively uncracked, the comparison of the observed modal frequencies with those of the gross section stiffness model showed quite a good match, albeit with the model predicting slightly higher frequencies. Fig. 11 clearly shows the reduction in natural frequencies with increased shaking intensity as the elements progressed from the initial uncracked section stiffness to the cracked section stiffness. Eventually, a further reduction

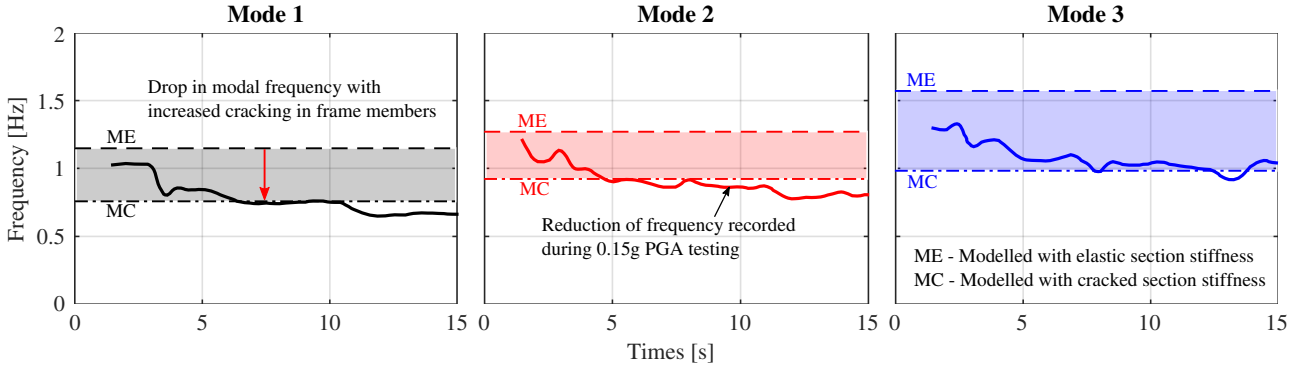

Fig. 11. Comparison of modal properties for gross and cracked section stiffness models with evolution of actual modal properties with increased damage during testing at $0.15g$ peak ground acceleration intensity on SPEAR test specimen reported by Negro (2005) and O'Reilly and Sullivan (2017a).

in natural frequency due to the initiation of damage to the members occurred. This reduction in natural frequency between the beginning and end of the test was less than 1 Hz for all three modes.

Other sources of lateral stiffness in RC buildings include nonstructural elements such as light and heavy interior partitions, which were not modeled explicitly in the numerical models and may account for some of the discrepancy. The masonry infills, however, were modeled fully and their behavior examined further. As previously described, the masonry infills were modeled using an equivalent diagonal strut model approach (Crisafulli et al. 2000). The hysteretic backbone outlined by Sassun et al. (2015) was adopted and was based on a modification of a previous proposal by Decanini et al. (2004) that uses mechanical properties provided by Hak et al. (2012) to compute the various parameters of the hysteretic backbone. Sassun et al. (2015), however, collected detailed data from almost 100 different test specimens reported in the literature and identified the exceedance of a number of defined damage states of the infill. This information was then used as a basis to modify the original deformation values for the hysteretic backbone proposed by Decanini et al. (2004), where this modification was intended to produce a modeling approach more representative of the physical observations of damage during testing. The Sassun et al. (2015) model may be considered representative of the infill panel's cracked behavior following some initial cycles of low-amplitude loading and is more flexible than that outlined initially by Decanini et al. (2004). As such, the cracked section stiffness of the infill panels was computed using the information provided by Sassun et al. (2015) because it is based on actual test data, whereas the panel uncracked section stiffness was computed from principles of mechanics using the material properties provided by Hak et al. (2012). Ricci et al. (2011) highlighted the impact that the condition of the masonry infill (i.e., cracked or uncracked) can have on empirical expressions to estimate the elastic period of RC frames buildings with masonry infill. Perrone et al. (2016) also noted the influence of the mechanical (Young's modulus) and geometric properties (openings) of masonry infills on the estimation of the elastic period of masonry-infilled RC buildings.

In the case of the URM school buildings, two of the pertinent modeling parameters that were identified to significantly influence the modal properties of the buildings were the assumption of a cracked stiffness for the structural elements and the Young's modulus of the masonry. Building codes such as the Italian National Code (NTC 2008) and Eurocode 8 (CEN 2004) suggest taking the progressive stiffness degradation during cyclic loadings in masonry buildings into account by reducing the initial elastic stiffness. If detailed information about the behavior of the masonry after first cracking is not available, a reduction of the elastic stiffness equal to 50% is recommended. In TreMuri, a stiffness reduction factor was introduced to take the cracked conditions of the panels into account. This stiffness reduction factor was a function of the compressive stress state and was calibrated for two different levels of the nonlinear masonry behavior (Lagomarsino et al. 2013). The Avola masonry school building analyzed in this study was not damaged by previous earthquakes and there was no sign of degradation of the masonry. As such, the influence of the reduction factor of the masonry elastic stiffness on the vibration modes was investigated. A second meaningful consideration is related to the mechanical properties of the masonry. As reported by Magenes (2006), the direct experimental evaluation of the material mechanical properties is not always feasible. Depending on the quality and texture of the masonry, the estimation of the main mechanical properties could often require destructive testing of panels of significant dimensions. The mechanical properties of masonry may tend to possess a large variability (Hendry 1990; Tomaževič 2009), which could significantly affect the results both in terms of elastic period and capacity. In the Avola school building analyzed here, it was not possible to perform destructive in situ measurements, and hence the mean value of the Young's modulus proposed in the literature for the same masonry typology was adopted (NTC 2008; CEN 2004; Tomaževič 2009). Based on this, it was evident that the parameter most affecting the modal properties was, in fact, the Young's modulus of the masonry. In the parametric study, this value was varied between 1,000 and 3,000 MPa, resulting in the first natural frequency of vibration varying between 2.94 and 6.25 Hz. The same consideration was pointed out by Aras et al. (2011), who varied the Young's modulus to match the elastic frequency recorded during ambient vibration survey. Aras et al. (2011) pointed out that if the numerical models accurately reproduce the geometry of the building, the main parameter affecting the evaluation of the elastic frequency is the Young's modulus of the masonry, a finding consistent with the present study.

Lastly, in the case of the Cassino precast school building, the use of cracked stiffness and the influence of cladding and partitions were identified as the factors most likely to influence the natural frequencies. The moments of inertia of the beams and columns were changed from their effective values (allowing for cracking) to their gross values. The building was clad in a lightweight precast concrete cladding system, which was not incorporated into the initial model. Each cladding panel spanning from ground to roof level was modeled as an elastic frame element for the purpose

Table 3. Stiffness ranges used in original and revised models for various elements used in each school building

Member	Model	Ancona	Carrara	Avola	Cassino
RC columns (section stiffness)	Original	$0.09–0.33EI_{gross}$	$0.18–0.39EI_{gross}$	—	$0.20–0.40EI_{gross}$
	Revised	EI_{gross}		—	EI_{gross}
RC beams (section stiffness)	Original	$0.10–0.15EI_{gross}$	$0.09–0.10EI_{gross}$	—	$0.10–0.15EI_{gross}$
	Revised	EI_{gross}		—	EI_{gross}
Masonry infills (panel lateral stiffness)	Original	$F_{DS1}/\theta_{DS1}H$		—	—
	Revised	$E_{w\theta}Bt_w/H$		—	—
URM stiffness	Original	—	—	ηEI_{gross}	—
	Revised	—	—	EI_{gross}	—

of eigenvalue analysis. Finally, interior masonry infill partition walls were incorporated into the model using the same modeling approach as for the RC frames. Also investigated was whether the diaphragm flexibility influenced the dynamic response of the structure; however, its influence was negligible when evaluated against a rigid diaphragm assumption.

For each of the school buildings, Table 3 provides the stiffness ranges used in the various elements between the original and revised models. For the RC frame members, EI_{gross} refers to the gross section stiffness. For the masonry infill models, B and H refer to the bay width and story height, respectively. The terms F_{DS1} and θ_{DS1} refer to the lateral force and drift at Damage state 1 computed using the expressions outlined by Sassun et al. (2015). The terms t_w and $E_{w\theta}$ refer respectively to the masonry infill panel thickness and to the elastic modulus computed as a function of the vertical and horizontal elastic moduli and the angle of the equivalent diagonal strut using the expressions outlined by Decanini et al. (2004). For the URM building, a stiffness-reduction coefficient (η) accounting for the panel cracked conditions was considered in the original model (Lagomarsino et al. 2013). This reduction coefficient was a function of the axial load acting on the panels and was calibrated by means of parametric nonlinear FEM analyses; η was assumed to be equal to 1 in the revised model. For the PC building, the RC frame members were modified in the same way as the RC building, and the cracked section stiffness ranges are indicated.

Revised Comparison with Ambient Vibration Measurements

With these revised numerical models of the four school buildings considered, the predicted modal properties were again compared with the measured ambient vibration values in Table 3. The measured:predicted natural frequency ratios improved drastically, with the models having a much higher natural frequency for each mode. However, there was still a small discrepancy between the predicted and measured frequencies. This may be attributed, in part, to the lack of explicit modeling of some of the nonstructural elements. In addition, for the Avola masonry building, the assumption of cracked section stiffness was deemed to be inadequate for the evaluation of the modal properties. Considering a Young's modulus equal to 1,500 MPa, a value corresponding closely to the average value proposed by the codes (NTC 2008; CEN 2004), the measured:predicted ratio of the natural frequencies improved further. The variation of the Young's modulus and the assumption of uncracked section stiffness were combined in the same model. With these values, the numerical model matched the measured frequencies from the in situ instrumentation. For the Cassino precast building, the use of gross section properties increased the fundamental frequency by approximately 30%. The incorporation of cladding panels and partitions then resulted in further increases of the fundamental frequency by 90% and 20%, respectively. Despite the significant increase in stiffness, the discrepancies for the precast building were still relatively large, although the lack of quality information from the data acquisition system is noted as a limiting factor.

Triggered Response from 2016 Central Italy Earthquake

The accelerometers installed in each building recorded not only the ambient vibrations but also the building response if triggered during a seismic event. Such an event occurred in Central Italy in August 2016, where at 02:36 Central European Time the instruments in the Ancona RC school building were triggered by the M6.0 earthquake that occurred approximately 100 km from the school (INGV 2017). Fig. 12 shows the two components of the motion recorded at both the base and the roof of the building and the acceleration response spectra. The recorded peak ground acceleration and peak roof acceleration were 0.037 and 0.118 g in the longitudinal direction and 0.032 and 0.070 g in the transverse direction, respectively; the amplification of the roof accelerations at certain frequencies with respect to the ground accelerations is evident. Two further aftershocks occurred in the days following the main event to again trigger the recording system.

Using the triggered recording of the building's response during each event, the natural frequencies approximated from the triggered shaking and those predicted by the blind and calibrated numerical models of the Ancona school were compared. The intensity of the ground motions was not high enough to cause any yielding in the school building, because when applied to both the initial and revised numerical models, the maximum peak story drifts remained less than 0.1% in both cases. However, it is reasonable to expect that during such shaking the structure's modal response would be more representative because the structure was being engaged more by a much stronger ground motion with respect to the intensity of the ambient vibration measurements.

In order to identify the modal properties during the triggered vibration, the acceleration recordings at both the ground and the roof of the building were examined to compute their transfer function. Because significant noise was observed in the raw signal recordings, especially at higher frequencies (i.e., >10 Hz), Welch's averaged, modified periodogram method of spectral estimation (Welch 1967) was used to smoothen the computed transfer functions using 300 overlaps of 500 windows using MATLAB version 8.4.0. Fig. 13 plots these amplitude transfer functions for each triggered vibration on a semilog scale. At the roof level, a second instrument placed at one end of school building was also used, and is labelled END, whereas the instrument positioned at the center of mass is labelled COM. Using this information, the natural

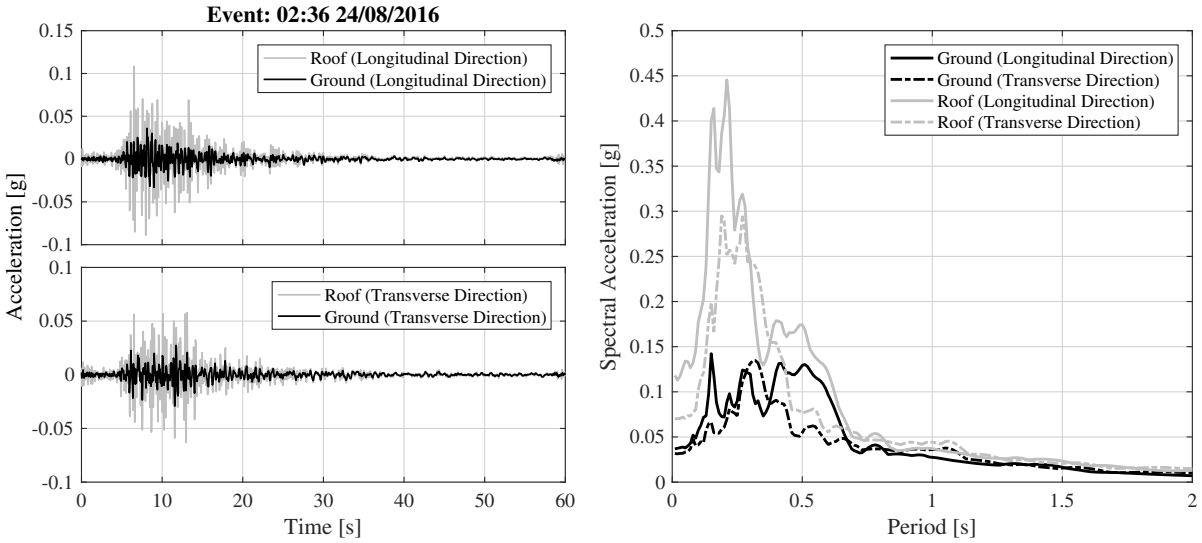

Fig. 12. Acceleration history and spectra of two components recorded during August 24, 2016 earthquake event at RC school building in Ancona.

frequencies were identified from the consistent amplifications in each of the transfer functions for each of the triggered recordings. Although this approach may be somewhat open to interpretation, the fact that three separate input signals were used and exhibited the same amplifications at the same frequencies argues that this is a reasonable method of estimating the modal properties within the scope of this study. Fig. 13 shows that the use of the acceleration recordings at the end of the school building was key in identifying the modal properties in the transverse direction. These corresponded to the lateral-torsional modes of vibration that otherwise would have been difficult to confidently identify by using just the COM recording. These differences in the transfer function (Fig. 13) between the two instruments positioned at different locations of the school building are to be expected considering the lateral-torsional behavior of the building outlined in Table 2 and the placement of the instruments at different ends of the building.

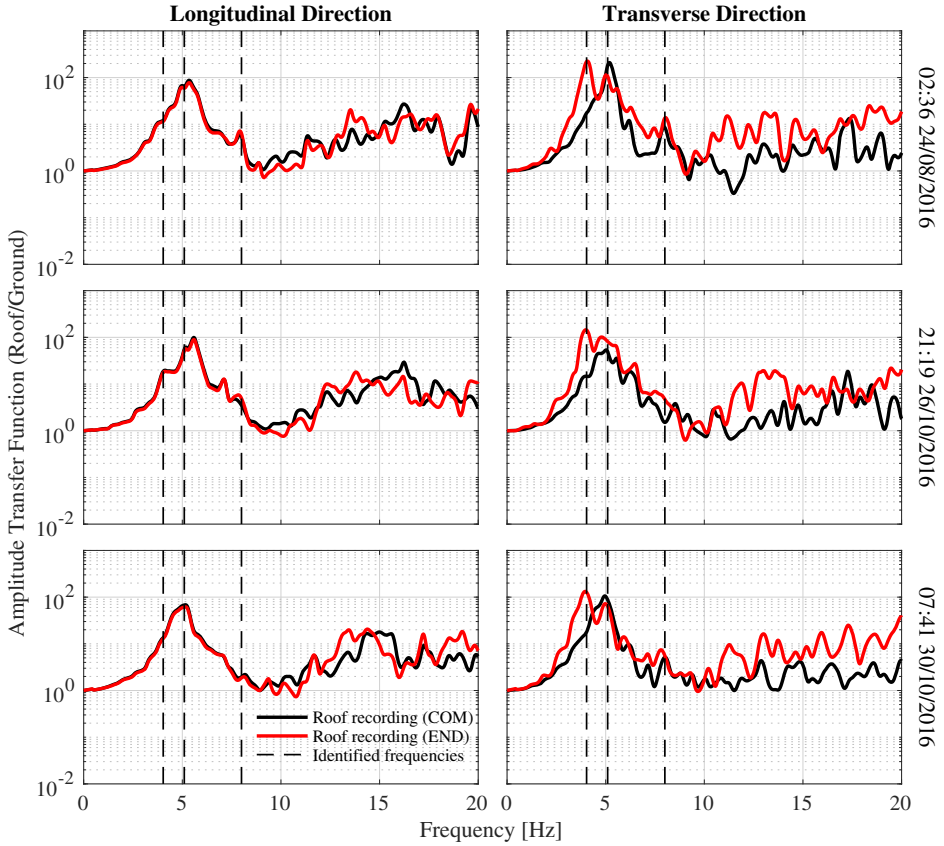

Fig. 13. Identification of modal periods of building using transfer functions for all three triggered vibrations recorded.

Table 4. Natural frequencies reported from ambient vibration measurements and predicted using revised numerical modeling

School	Mode	Mode shape	Natural frequency (Hz)		Measured/ revised prediction
			Revised prediction	Measured	
Ancona	1	Translational	3.66	5.25	1.4
	2	Lateral-torsional	5.28	6.38	1.2
	3	Translational	6.50	9.63	1.5
Carrara	1	Translational	4.05	4.50	1.1
	2	Lateral-torsional	6.68	5.13	0.8
	3	Lateral-torsional	7.46	6.38	0.9
Avola	1	Lateral-torsional	5.13	5.21	1.0
	2	Lateral-torsional	9.86	17.5	1.7
Cassino	1	Lateral-torsional	2.48	7.5	3.0
	2	Lateral-torsional	2.66	17.8	6.7

The modal properties during the triggered response were then computed, and the identified natural frequencies are listed in Table 4. It is immediately obvious when comparing the triggered and ambient vibration natural frequencies that there was a consistent decrease of approximately 20% in the triggered frequencies of the ambient vibration frequencies, meaning that the triggered response of the Ancona school building was more flexible. This was quite a significant decrease in natural frequencies, and is of interest here because when comparing these triggered vibration values to those of the revised modeling, the comparison in Table 5 shows better alignment with the model prediction. Overall, this observation gives a further degree of confidence that the revised numerical modeling indeed represented the initial uncracked stiffness of the school building quite well.

In addition, Fig. 14 compares the predicted roof acceleration response spectra and the actual roof spectra recorded during the triggered vibration at the Ancona school. This is a valuable comparison because it illustrates how the response of different modes of vibration of both the numerical models and actual building filter the same input ground motion to the roof level of the structure. Comparing the roof spectra predicted by the original numerical model with those of the instrument recording at the roof level, it is immediately clear that the assumption of cracked section stiffness for low-amplitude vibrations is not adequate. This is apparent from the elongated peak periods and their corresponding spectral peaks compared with the observed roof spectra of the building. This is particularly notable in the longitudinal direction, in which the peak amplitude of the roof spectra of the original models was markedly higher than that observed in the actual building. Comparing this with the revised model, in which the matching between the predicted and observed roof spectra was much better, not only were the peak amplitude of the floor spectra similar, but the identified modal properties tended to match very well also. In addition, the overall spectra away from the identified modal periods also tended to match reasonably well to give further confidence to the revised modeling approach outlined previously.

Implications of Numerical Modeling for Assessment of Structural Response

The previous sections highlighted the sensitivity of modal properties to assumptions in the numerical model. These observations are of great interest in seismic design and assessment because they highlight apparent inconsistencies between what a seismic engineer may implement in their numerical models and what is actually recorded when the building is instrumented. This section further investigates the relative impact of such disparities, not only in the initial phase of response with relatively little damage, but also at much higher intensities that push the structure past the initial elastic phase to the point of extensive damage.

A simple incremental dynamic analysis (IDA) was conducted for two modeling variations of the school building in Ancona to examine the impact on the building's story drift and floor acceleration demands with respect to increasing intensity. The two models of the school were identical with the exception of their assumptions regarding initial stiffness, which incorporated the observations of the preceding parametric study to examine the effects of the RC frame member and masonry infill initial stiffness assumptions. Fig. 15 illustrates the two modeling approaches, in which the member properties were modified to initially behave as fully elastic members with gross section stiffness and possess the ability to crack and reduce their section stiffness for the subsequent cycles of response. This was implemented in OpenSees using the Parallel material aggregator so that the member hysteretic behavior had an additional elastic material with finite deformation capacity defined using the MaxMin material model available in OpenSees. For the RC frame elements, for example, the additional material model with stiffness equal to the difference in the gross (EI_{gross}) and the cracked (EI_{cr}) section stiffnesses was then added to the existing cracked section stiffness element model to give an element with initial stiffness equal to EI_{gross}. If the flexural demands exceeds the flexural cracking strength, M_{cr}, this additional stiffness is lost and the member stiffness returned to that of EI_{cr} [Fig. 15(a)]. In the case of the cracking strength of the element, the element stiffness decreases and behaves as a cracked member from that instant onward in the dynamic analysis. This was deemed to be representative of how RC frame members behave in reality. In practice, however, numerical modeling typically adopted in seismic design and assessment is more concerned with the postyield and collapse behavior of structures, and therefore tends to ignore this for simplicity. The flexural cracking strength, M_{cr}, of the RC frame members was determined following the expressions outlined by Collins and Mitchell (1991) to determine the tensile strength of concrete, and from sectional analysis returned a flexural strength.

In the case of the equivalent diagonal strut modeling of the masonry infills, the initial stiffness illustrated in Fig. 15(b) was

Table 5. Natural frequencies reported from triggered vibration measurements and predicted using both initial and revised numerical modeling approaches

Mode	Mode shape	Natural frequency (Hz)				Triggered/ ambient	Triggered/ initial prediction	Triggered/ revised prediction
		Initial prediction	Revised prediction	Ambient	Triggered			
1	Translational	1.61	3.66	5.25	4.0	0.77	2.50	1.09
2	Lateral-torsional	2.24	5.28	6.38	5.1	0.80	2.28	0.97
3	Translational	2.74	6.50	9.63	8.0	0.83	2.92	1.23

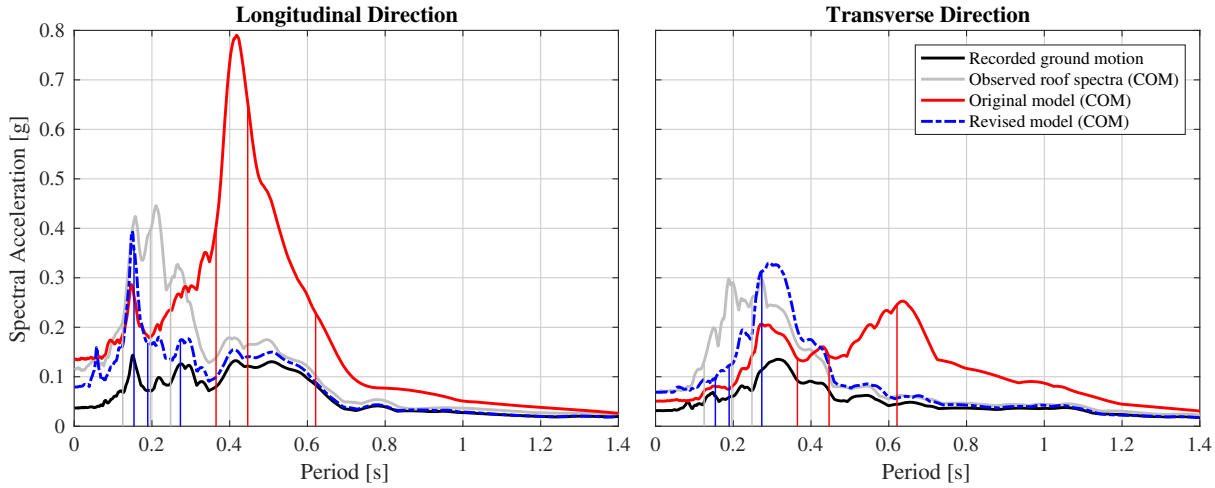

Fig. 14. Comparison of 5% damped roof spectra recorded during triggered vibration and spectra predicted using initial and revised models. Vertical lines are the identified modal periods.

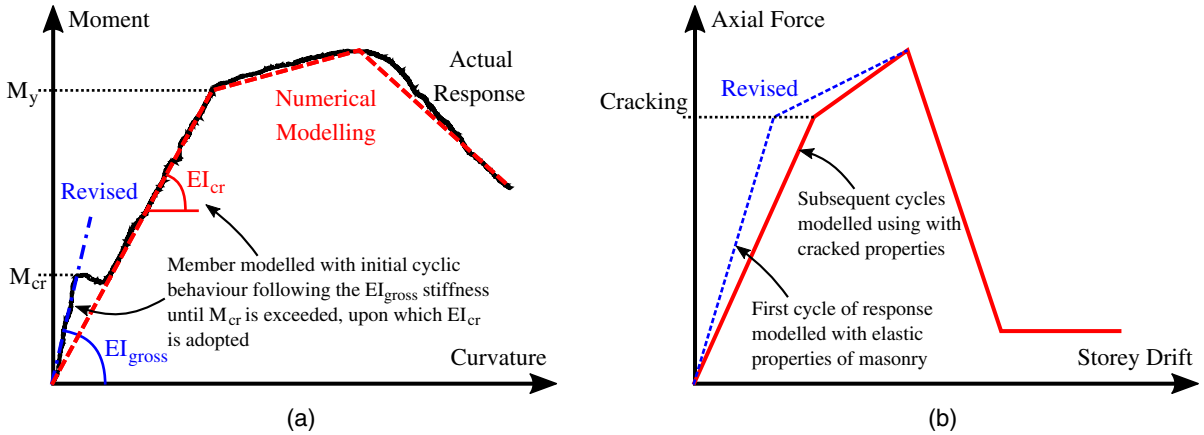

Fig. 15. Modifications to RC frame member and masonry infill equivalent diagonal strut hysteretic properties to examine the impact of incorporating initial uncracked stiffness on seismic response of school building in Ancona: (a) RC frame members; and (b) masonry infill equivalent status.

modified in a similar fashion. The initial stiffness was modified to equal that determined using the approach outlined by Dolsek and Fajfar (2008) that computes the initial stiffness based on the characteristic material properties. Upon the exceedance of the cracking strength of the masonry infill computed using the approach outlined by Decanini et al. (2004), the stiffness of the strut elements was reduced to that proposed by Sassun et al. (2015), which may be considered more representative of the cracked behavior of the masonry infill.

With this approach, the RC frame members and masonry infill diagonal struts were crackable elements with initial stiffness properties of an elastic model and a postcracking behavior equal to what is typically adopted from the outset of analysis. This revised model with crackable section stiffness was compared with the initial numerical model (Fig. 5) in terms of both story drift and floor acceleration demand. The ground motion recorded at the base of the school building in Ancona during the triggered earthquake event was used to perform a simple IDA of both building models and illustrate the relative impacts. Fig. 16 illustrates the IDA response, reporting the maxima of both the peak story drift and the peak floor accelerations (PFAs) with respect to increasing intensity of the single ground motion. The intensity measure adopted here was the peak ground acceleration due to its independence of the modal properties. Unlike the spectral acceleration at the first-mode period, $Sa(T_1)$, which is typically adopted (FEMA 2012), it allows for a more direct comparison between the two models. Fig. 16 also plots the observed PFA from instruments during the triggered vibration to highlight how this observed value matches the results of the numerical model. Furthermore, the response of the structure was compared with the predictions of the N2 method for infilled frames (Dolšek and Fajfar 2005). The responses of the initial and revised models converged toward one another, and were quite similar considering the approximations of the N2 method and the complexity of the structure.

Fig. 16 shows how the responses were somewhat similar in terms of the general magnitude, with the initial model exhibiting a slightly higher drift demand and lower floor accelerations. This is an expected result due to the increased flexibility of the model, and in turn resulted in an increase in drift and reduced the floor accelerations in the building. Examining the ratios of response at the different intensities, the subplots adjacent to both the peak story drift and peak floor acceleration illustrate the ratio of the demands

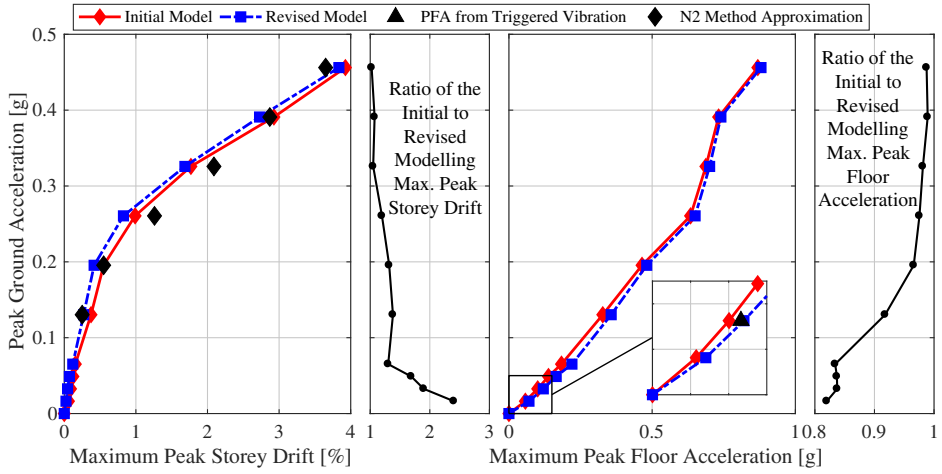

Fig. 16. Ancona school building's response to signal recorded at building during 2016 earthquake using IDA adopting both cracked (initial model) and initially uncracked (revised model) section stiffness models for RC frame and masonry infill elements.

for the initial and revised models. As anticipated, the initial model showed a much larger drift demand because the ratios for low seismic intensities were more than 2 times greater than those of the revised model. As the intensity increased, the presence of the initially uncracked section stiffness in the numerical models became less significant as the ratio approached unity. Similarly, in the case of the floor accelerations, the ratios of the cracked model to the initially uncracked were around 0.85 for low intensities but gradually approached unity with increasing intensity. Lastly, the intensity at which the responses of the cracked and initially uncracked models began to converge (Fig. 16) corresponded to approximately $0.10g$ peak ground acceleration. Although it would be useful to identify an intensity level at which the effects of cracked versus initially uncracked section stiffness are negligible, such a value cannot be reliably determined from a single ground motion record alone, because other factors such as frequency content and record duration, in addition to the magnitude, distance, and spectral shape characteristics with respect to the local seismic hazard disaggregation, would also be expected to play a significant role in the determination of such an intensity.

Discussion

From the previous sections, some general comments can be made on the overall impact on future seismic assessment and loss estimation studies. The first point worth commenting on is the accuracy of the numerical modeling for the different structural typologies. Comparing the measured and numerically predicted modal properties highlighted how the initial comparison of modal properties significantly differed in terms of their natural frequencies, with the predicted value being much lower than those determined from ambient vibration, suggesting that the numerical models were too flexible. This difference alone would question whether the numerical models themselves are representative of the actual building response. Because each model was built using data collected from in situ inspection, a degree of confidence was maintained in each model's predictive capability. This was further bolstered by the fact that the numerical models identified similar mode shapes as those established from the instrumentation placed at each school building following inspection, which suggests that the relative distributions of mass and stiffness throughout the buildings' plans and elevations were representative. As such, these differences were identified as an individual member stiffness issue, and the parametric study showed that adopting different values of member stiffness, considering that the different building components may be responding in its elastic, uncracked range of response, significantly improved the comparisons of ambient vibrations measurements and numerical models. Therefore, although these models were developed with extensive NRHAs over the full range of response in mind, their application to analysis in the initial stages of structural response warrants further consideration. Furthermore, although modal analysis results provide useful information regarding a structure's dynamic behavior, the comparison and parametric studies presented so far are intended to form the basis of furthering the general discussion and do not necessarily imply that modal analysis alone should be used to calibrate numerical models.

This led to another consideration: if these numerical models are not appropriate for analyses over the full range of structural response, what implication does this have on loss estimation studies that require structural response characterization during both rare and more-frequent earthquake events? In terms of story drift, the models that adopt cracked initial section stiffness tend to overestimate the peak drift demands at each floor at lower shaking intensity. On the other hand, the same model would tend to underestimate the peak floor accelerations along the height of the building. The two models tended to converge at the intensity inducing around 0.15% peak story drift and $0.20g$ peak floor acceleration (Fig. 16). This level of demand is not likely to induce any damage in the structural members; Cardone (2016) reported a median drift of 0.95% for the limit state inducing first cracking in slender nonductile columns, for example. For nonstructural elements, however, these tend to have a much lower initiation threshold and would be expected to influence their damage and expected repair costs. However, because the difference in modeling assumptions tends to increase the expected drift but decrease the floor accelerations at these lower intensities, no single trend or bias is introduced in the expected losses (i.e., expected losses will not always be higher or lower than if these model refinements had not been considered), but rather an amplification in the dispersion of losses due to increased modeling uncertainty. Although the absolute values of drift and floor acceleration may be small and their uncertainty relatively low compared with other, more-severe limit states, their impact on the computation of annualized losses through integration with the seismic hazard curve could be a useful exercise to investigate in the future.

J. Perform. Constr. Facil., 2019, 33(1): 04018089

The initial behavior and overall performance of the structure are of paramount importance, because this corresponds to the region of the seismic hazard curve that is weighted more heavily during the hazard integration due to the higher mean annual frequency of exceedance for lower intensity events. However, the point at which the model is better represented using cracked section stiffness from the outset may, in fact, correspond to return periods equal to or greater than those typically considered in seismic assessment (e.g., >50 years). A potential solution to this was outlined, whereby RC frame and masonry infill elements were modeled using initial uncracked section stiffness up to a certain value of deformation, after which the members were deemed to have cracked and the element stiffnesses reverted to those of the cracked section stiffness typically used in seismic assessment. Comparing the IDA response curves for the ground motion recorded during the 2016 Central Italy earthquake in the school building illustrated the discrepancy between the response of the two modeling approaches at low intensities. It also showed that the responses of both models converged toward each other upon sufficient damage to the structure, so that the assumption of cracked section stiffness also becomes representative. Although this is beyond the scope of this paper, it is an area that ought to be studied, as in O'Reilly and Sullivan (2018a), for example, to examine the potential impacts of the modeling decisions in the elastic range on the estimation of monetary losses.

Summary and Conclusions

This paper examined the system identification of a number of existing school buildings of different structural typologies identified as being representative of the general population located throughout Italy. Ambient vibration measurements at each school allowed the modal properties to be established and subsequently compared with numerical predictions. Although the comparison in terms of mode shape was good, suggesting that the overall relative distribution of mass and stiffness in the numerical models was adequate, the matching in terms of natural frequency was somewhat poor, with the numerical models tending to be too flexible. Parametric studies were conducted, and in the case of the RC frame buildings with masonry infill, the assumption of a cracked section stiffness for both the frame members and the masonry infill modeling was identified as the cause of such a discrepancy. In the case of the unreinforced masonry building, similar analysis demonstrated that the Young's modulus adopted was critical. The monitoring systems were also set up to be triggered and to record in the event of an earthquake, which occurred during the 2016 Central Italy earthquake near the school building in Ancona. Comparison of the natural frequencies identified during the triggered event and the ambient vibration showed similar mode shapes but a constant reduction in the natural frequency of around 20%. Comparing the triggered values with those predicted using the numerical model showed quite a good match when considering the uncracked stiffness of the structural elements. Using this triggered earthquake response, a comparative study was conducted to examine the impact of considering a modeling approach, whereby the RC frame and equivalent diagonal masonry strut stiffnesses were modeled as initially elastic, with the ability to switch the cracked section stiffness for the remainder of the analysis should the cracking strength be exceeded. An incremental dynamic analysis was conducted on both models to examine the impacts on response. The cracked section stiffness model tended to overestimate peak story drifts and underestimate peak floor accelerations at lower intensities before both converging to the same peak response. Lastly, some of the implications of the different observations presented in this paper were discussed within the broader context of seismic assessment.

Overall, some important considerations can be drawn from the system identification presented here within the broader framework of seismic assessment of existing structures:

- Modal properties identified during the triggered vibration recording at the school building in Ancona were compared with the ambient vibrations, and showed a constant reduction in modal frequencies by around 20%. This is significant because it not only aligns much better with the predictions of the numerical model but also highlights that the modal properties are also sensitive to the intensity of input shaking, in which the-more engaging triggered response values may be considered more representative.
- Using cracked stiffness models was shown to be appropriate in seismic assessment in which the full range of response is examined, but it misrepresented the initial modal properties compared with ambient vibration measurements.
- Furthermore, comparing the responses of the two numerical modeling approaches, one of which was modeled with uncracked section stiffness and was permitted to decrease once its cracking strength was exceeded, the responses in terms of peak story drift and floor acceleration approaches converged toward the cracked member stiffness model as intensity increased. Therefore, the impacts of the initial uncracked section stiffness on the overall response of the structure at upper response limit states and eventual complete collapse are not likely to be affected by omitting this initial behavior.
- Misrepresenting the initial elastic behavior of structures using cracked section stiffness models does, however, lead to an overestimation of peak drift demand and lower floor accelerations during more-frequent earthquakes. Identifying the intensity levels below which the consideration of the initial uncracked behavior of the members is necessary was discussed and noted as being a possibility for future parametric studies.

Considering the above points derived using the data collected and analyzed as part of this paper, practitioners should take care to ensure that their structural models are indeed representative over the range of structural response of interest. Discrepancies in the initial range of structural response may have a significant impact on the computation of expected annual losses, which tend to be heavily weighted by contributions from frequent, low-intensity earthquakes.

Acknowledgments

The authors acknowledge the funding provided by the Centro di Geomorfologia Integrata per l'Area del Mediterraneo (CGIAM) and the European Centre for Training and Research in Earthquake Engineering (EUCENTRE). The authors also acknowledge the help of Matteo Moratti and Barbara Borzi, who assisted in the in situ surveying of the school buildings, and Fernando Bastos, who contributed to the postprocessing of the triggered recording of the building's response during the Central Italy Earthquake.

References

Aras, F., L. Krstevska, G. Altay, and L. Tashkov. 2011. "Experimental and numerical modal analyses of a historical masonry palace." *Constr. Build. Mater.* 25 (1): 81–91. https://doi.org/10.1016/j.conbuildmat.2010.06.054.

Bacco, V. 2009. "Solaio in latero-cemento: Confronto con sistemi alternativi." Accessed October 15, 2018. http://download.acca.it/BibLus-net/VecchiAllegatiBiblus/Approfondimenti_Tecnici/ConfrontoAlternativiANDIL_58.pdf.

Bonetto, A. 2013. "Sviluppo e applicazione di algoritmi per l'identificazione dinamica e il rilevamento del danno delle strutture civili." Tesi di Laurea Magistrale, Dipartimento di Ingegneria civile, edile e ambientale, Università degli Studi di Padova.

Borzi, B., P. Ceresa, M. Faravelli, E. Fiorini, and M. Onida. 2011. "Definition of a prioritization procedure for structural retrofitting of Italian school buildings." In *Proc., 3rd ECCOMAS Thematic Conf. on Computational Methods in Structural Dynamics and Earthquake Engineering*. Corfu, Greece.

Cardone, D. 2016. "Fragility curves and loss functions for RC structural components with smooth rebars." *Earthquakes Struct.* 10 (5): 1181–1212. https://doi.org/10.12989/eas.2016.10.5.1181.

Carr, A. J. 2007. *RUAUMOKO—User manual, theory, and appendices*. Christchurch, New Zealand: Dept. of Civil and Natural Resources Engineering, Univ. of Canterbury.

CEN (European Committee for Standardization). 2004. *Eurocode 8: Design of structures for earthquake resistance. Part 1: General rules, seismic actions and rules for buildings*. EN 1998-1:2004. Brussels, Belgium: CEN.

CEN (European Committee for Standardization). 2005. *Eurocode 8: Design of structures for earthquake resistance. Part 3: Assessment and retrofit of buildings*. EN 1998-3:2005. Brussels, Belgium: CEN.

Collins, M. P., and D. Mitchell. 1991. *Prestressed concrete structures*. Englewood Cliffs, NJ: Prentice Hall.

Crisafulli, F. J., A. J. Carr, and R. Park. 2000. "Analytical modeling of infilled frame structures—A general review." *Bull. N. Z. Soc. Earthquake Eng.* 33 (1): 30–47.

Decanini, L., F. Mollaioli, A. Mura, and R. Saragoni. 2004. "Seismic performance of masonry infilled R/C frames." In *Proc., 13th World Conf. on Earthquake Engineering*. Vancouver, BC, Canada.

Dolšek, M., and P. Fajfar. 2005. "Simplified non-linear seismic analysis of infilled reinforced concrete frames." *Earthquake Eng. Struct. Dyn.* 34 (1): 49–66. https://doi.org/10.1002/eqe.411.

Dolšek, M., and P. Fajfar. 2008. "The effect of masonry infills on the seismic response of a four-storey reinforced concrete frame—A deterministic assessment." *Eng. Struct.* 30 (7): 1991–2001. https://doi.org/10.1016/j.engstruct.2008.01.001.

FEMA. 2012. *Seismic performance assessment of buildings: Volume 1—Methodology (P-58-1)*. FEMA P58-1. Washington, DC: FEMA.

Hak, S., P. Morandi, G. Magenes, and T. J. Sullivan. 2012. "Damage control for clay masonry infills in the design of RC frame structures." Supplement, *J. Earthquake Eng.* 16 (S1): 1–35. https://doi.org/10.1080/13632469.2012.670575.

Hendry, A. W. 1990. *Structural masonry*. London: Macmillan Education.

INGV (Istituto Nazionale di Geofisica e Vulcanologia). 2017. "Lista dei terremoti aggiornata in tempo reale dal Centro Nazionale Terremoti. Monitoraggio e sorveglianza sismica in Italia." Accessed March 21, 2017. http://cnt.rm.ingv.it/.

Islami, K. 2013. "System identification and structural monitoring of bridge structures." Ph.D. thesis, Dipartimento di Ingegneria civile, edile e ambientale, Università degli Studi di Padova.

Lagomarsino, S., A. Penna, A. Galasco, and S. Cattari. 2013. "TREMURI program: An equivalent frame model for the nonlinear seismic analysis of masonry buildings." *Eng. Struct.* 56 (Nov): 1787–1799. https://doi.org/10.1016/j.engstruct.2013.08.002.

Magalhães, F., A. Cunha, and E. Caetano. 2012. "Vibration based structural health monitoring of an arch bridge: From automated OMA to damage detection." *Mech. Syst. Signal Process.* 28 (Apr): 212–228. https://doi.org/10.1016/j.ymssp.2011.06.011.

Magenes, G. 2006. "Masonry building design in seismic areas: Recent experiences and prospects from a European standpoint." In *Proc., 1st European Conf. on Earthquake Engineering and Seismology*. Geneva.

McKenna, F., M. H. Scott, and G. L. Fenves. 2010. "Nonlinear finite-element analysis software architecture using object composition." *J. Comput. Civ. Eng.* 24 (1): 95–107. https://doi.org/10.1061/(ASCE)CP.1943-5487.0000002.

Melo, J., H. Varum, T. Rossetto, and A. Costa. 2012. "Experimental response of RC columns built with plain bars under unidirectional cyclic loading." In *Proc., 15th World Conf. on Earthquake Engineering*. Lisbon, Portugal.

Molina, F. J., G. Verzeletti, G. E. Magonette, P. Buchet, and M. Géradin. 1999. "Bi-directional pseudodynamic test of a full-size three-storey building." *Earthquake Eng. Struct. Dyn.* 28 (12): 1541–1566. https://doi.org/10.1002/(SICI)1096-9845(199912)28:12<1541::AID-EQE880>3.0.CO;2-R.

Montaldo, V., and C. Meletti. 2007. "Valutazione del valore della ordinata spettrale a 1sec e ad altri periodi di interesse ingegneristico. Progetto DPC-INGV S1, Deliverable D3." Accessed March 21, 2017. http://esse1.mi.ingv.it/d3.html.

Negro, P. 2005. "Full-scale PSD testing of the torsionally unbalanced spear structure in the 'as-built' and retrofiitted configurations." In *Proc., SPEAR Int. Workshop: Seismic Performance Assessment and Rehabilitation of Existing Buildings*, edited by M. N. Fardis and P. Negro, 139–154. Ispra, Italy.

Negro, P., E. Mola, F. J. Molina, and G. E. Magonette. 2004. "Full-scale PSD testing of a torsionally unbalanced three-storey non-seismic RC frame." In *Proc., 13th World Conf. on Earthquake Engineering*. Vancouver, BC, Canada.

NTC (Norme Tecniche per le Costruzioni). 2008. *Norme Tecniche Per Le Costruzioni*. Rome: NTC.

O'Reilly, G. J. 2016. "Performance-based seismic assessment and retrofit of existing RC frame buildings in Italy." Ph.D. thesis, ROSE Programme, Centre for Understanding and Managing Extremes, Scuola Universitaria Superiore IUSS Pavia.

O'Reilly, G. J., R. Monteiro, D. Perrone, I. Lanese, M. J. Fox, A. Pavese, and A. Filiatrault. 2017. "System identification and structural modelling of Italian school buildings." In Vol. 2 of *Dynamics of civil structures*, edited by J. Caicedo and S. Pakzad. Cham, Switzerland: Springer.

O'Reilly, G. J., D. Perrone, M. Fox, R. Monteiro, and A. Filiatrault. 2018. "Seismic assessment and loss estimation of existing school buildings in Italy." *Eng. Struct.* 168 (Aug): 142–162. https://doi.org/10.1016/j.engstruct.2018.04.056.

O'Reilly, G. J., and T. J. Sullivan. 2015. "Influence of modelling parameters on the fragility assessment of pre-1970 Italian RC structures." In *Proc., 5th ECCOMAS Thematic Conf. on Computational Methods in Structural Dynamics and Earthquake Engineering*. Crete Island, Greece.

O'Reilly, G. J., and T. J. Sullivan. 2017a. "Modeling techniques for the seismic assessment of the existing Italian RC frame structures." *J. Earthquake Eng.* 1–35. https://doi.org/10.1080/13632469.2017.1360224.

O'Reilly, G. J., and T. J. Sullivan. 2017b. "Modelling uncertainty in existing Italian RC frames." In *Proc., 6th Int. Conf. on Computational Methods in Structural Dynamics and Earthquake Engineering*. Rhodes Island, Greece.

O'Reilly, G. J., and T. J. Sullivan. 2018a. "Probabilistic seismic assessment and retrofit considerations for Italian RC frame buildings." *Bull. Earthquake Eng.* 16 (3): 1447–1485. https://doi.org/10.1007/s10518-017-0257-9.

O'Reilly, G. J., and T. J. Sullivan. 2018b. "Quantification of modelling uncertainty in existing Italian RC frames." *Earthquake Eng. Struct. Dyn.* 47 (4): 1054–1074. https://doi.org/10.1002/eqe.3005.

Pampanin, S., G. M. Calvi, and M. Moratti. 2002. "Seismic behaviour of RC beam-column joints designed for gravity loads." In *Proc., 12th European Conf. on Earthquake Engineering*. London.

Paulay, T., and M. J. N. Priestley. 1992. *Seismic design of reinforced concrete and masonry buildings*. New York: Wiley.

Perrone, D., M. Leone, and M. A. Aiello. 2016. "Evaluation of the infill influence on the elastic period of existing RC frames." *Eng. Struct.* 123 (Sep): 419–433. https://doi.org/10.1016/j.engstruct.2016.05.050.

Piovesan. 2013. "Sistema di Identificazione Dinamica per Ponti: Sviluppo di Algoritmi Automici nel Dominio della Frequenza per Monitoraggi Continui." Tesi di Laurea Magistrale, Dipartimento di Ingegneria civile, edile e ambientale, Università degli Studi di Padova.

Priestley, M. J. N. 1993. "Myths and fallacies in earthquake engineering – Conflicts between design and reality." *Bull. N. Z. Soc. Earthquake Eng.* 26 (3): 329–341.

Priestley, M. J. N. 2003. "Myths and fallacies in earthquake engineering, Revisited." In *Proc., 9th Mallet Milne Lecture*. Pavia, Italy: IUSS Press.

Rainieri, C., G. Fabbrocino, and E. Cosenza. 2009a. "Identificazione dinamica autonoma, problemi e prospettive di applicazione al monitoraggio strutturale in zona sismica." In *Atti del 8 Convegno Nazionale ANIDIS*. Bologna, Italy.

Rainieri, C., G. Fabbrocino, and E. Cosenza. 2009b. "Fully automated OMA: An opportunity for smart SHM system." In *Proc., IMAC-XXVII*. Orlando, FL.

Ricci, P., G. M. Verderame, and G. Manfredi. 2011. "Analytical investigation of elastic period of infilled RC MRF buildings." *Eng. Struct.* 33 (2): 308–319. https://doi.org/10.1016/j.engstruct.2010.10.009.

SARA Electronic Instruments. 2018. "SARA SA10 datasheet." Accessed April 23, 2018. http://www.sara.pg.it/documents/commercial/SA10_DATASHEET_ENG.PDF.

Sassun, K., T. J. Sullivan, P. Morandi, and D. Cardone. 2015. "Characterising the in-plane seismic performance of infill masonry." *Bull. N. Z. Soc. Earthquake Eng.* 49 (1): 100–117.

SPIR (Seismic Project Identification Report). 2014. *Structural engineering guidelines for the performance-based seismic assessment and retrofit of low-rise British Columbia school blocks*. 2.1 ed. Canada: SPIR.

Tomaževič, M. 2009. "Shear resistance of masonry walls and Eurocode 6: Shear versus tensile strength of masonry." *Mater. Struct.* 42 (7): 889–907. https://doi.org/10.1617/s11527-008-9430-6.

Vincenzi, L. 2007. "Identificazione Dinamica delle Caratteristiche Modali e delle Proprietà Meccaniche di Strutture mediante Algoritmi di Ottimizzazione." Ph.D. thesis, Dipartimento di Ingegneria civile, Chimica, Ambientale e dei Materiali, Università degli Studi di Bologna.

Vona, M., and A. Masi. 2004. "Resistenza sismica di telai in c.a. progettati con il R.D. 2229/39." In *Proc., XI Congresso Nazionale 'L'Ingegneria Sismica in Italia*. Genoa, Italy.

Welch, P. 1967. "The use of fast Fourier transform for the estimation of power spectra: A method based on time averaging over short, modified periodograms." *IEEE Trans. Audio Electroacoust.* 15 (2): 70–73. https://doi.org/10.1109/TAU.1967.1161901.

Zimos, D. K., P. E. Mergos, and A. J. Kappos. 2015. "Shear hysteresis model for reinforced concrete elements including the post-peak range." In *Proc., 5th ECCOMAS Thematic Conf. on Computational Methods in Structural Dynamics and Earthquake Engineering*. Crete Island, Greece.